LAWRENCE
LIVERMORE
NATIONAL
LABORATORY

UCRL-JRNL-204066

X-ray Spectroscopy with Elliptical Crystals and Face-On Framing Cameras

R.F. Heeter, J.A. Emig, K.B. Fournier, S.B. Hansen, M.J. May, B.K.F. Young

May 24, 2004

Review of Scientific Instruments

X-ray Spectroscopy with Elliptical Crystals and Face-On Framing Cameras

R. F. Heeter, J. A. Emig, K. B. Fournier, S. B. Hansen, M. J. May, and B. K. F. Young

Lawrence Livermore National Laboratory

P.O. Box 808, L-472, Livermore, CA 94551

(Dated: May 24, 2004)

Abstract

X-ray spectrometers using elliptically bent crystals have desirable properties for applications requiring broad spectral coverage, good spectral resolution, and minimized source broadening. Previous work used custom-positioned film or microchannel plate detectors. We find it is also useful and cost-effective to field elliptical crystals in existing snouts on the face-on gated microchannel plate framing cameras commonly used at many facilities. We numerically explored the full design space (spectral range and resolution) of elliptical crystals compatible with the new MSPEC multipurpose spectrometer snout. We have tested at the Omega laser an elliptical RAP crystal with 174 mm focal length, 0.9885 eccentricity, and 4.6 degree inclination, viewing from 1.0 to at least 1.7 keV with E/dE of 300-500. A slit (2x mag) images 3 mm sources with 70 um spatial resolution.

PACS numbers: Valid PACS appear here

Elliptical crystal configurations have a variety of advantageous properties for broadband X-ray spectroscopy of extended sources [1, 2]. In the elliptical geometry, the source is at one focus, the crystal is bent in one direction along the surface of the ellipse (and flat in the other direction), and typically the detector is placed beyond the crossover point at the second focus. When crystals can be suitably bent and detectors placed suitably close to the second focus, a very wide range of Bragg angles is possible. In this geometry, extended sources are strongly demagnified, which reduces source broadening and improves spectral resolution. In fact there is a locus of points (one for each Bragg angle) where a Johann-type focusing of extended sources takes place [1, 3].

Until now, elliptical geometry apparently has only been used with detectors whose orientation (and curvature, for film packs) was customized for the instrument, with the detector plane roughly parallel to the axis of the ellipse, i.e. edge-on to the source [1–4]. However, for gated space-resolved spectroscopy on large lasers, the optimal (and reliable) detector is the pulsed microchannel plate, and these have been standardized with the plate essentially perpendicular to the laser-heated source (face-on) because of their widespread use in pinhole imaging. Rather than engineer an entirely new detector at great expense, we have instead evaluated the range of ellipses compatible with the available face-on detector geometry.

The geometry for this case is summarized in Fig. 1. The four critical parameters are the ellipse's eccentricity (ϵ) and focal length (f), the length of the detector L_d, and the inclination (η) of the ellipse's axis relative to the detector-source centerline. The inclination angle and focal length must be large enough relative to L_d that straight-through light can be blocked ($f \sin(\eta) > L_d/2$), but small enough that the crystal can be mounted within the space envelope available for the diagnostic. If the detector standoff distance is constrained, this also places an upper bound on the focal length, $2f < L_d$. The eccentricity is bounded on the low side by the diagnostic space envelope, and on the high side by the minimal allowed radius of curvature to which the desired crystal can be bent.

We now focus on the specific case of the standard X-Ray Framing Camera (XRFC) at the Omega laser. We have recently designed a multipurpose spectroscopy snout (MSPEC) which mounts on the XRFC and provides the maximal internal volume for mounting crystals, consistent with the standard diagnostic space envelope (which avoids all beam and diagnostic interferences) [5]. The diagnostic space envelope is defined as a cone starting 40.64 mm from the source and extending away from the source with a half-angle of 16 deg.

We have evaluated the entire range of MSPEC-compatible ellipses for both 2x and 3x magnification by means of a numerical scan over the $\epsilon - f - \eta$ configuration space. Scripts were written within the MATLAB software environment. For each configuration, the elliptical crystal and detector were respectively discretized on a 1 micron and 20 micron grid. All X-ray paths leading from source, through slit, off crystal, and into the detector were computed to determine the spectral coverage and resolution. Configurations incompatible with the XRFC (strip length $d \geq 30$mm, standoff $L_d = 381$ mm) were rejected. The spectral resolution arising from source broadening ($E/\Delta E_s$, assuming a 300 micron source) and detector spatial resolution ($E/\Delta E_d$, assuming 60 microns) were computed, along with the crystal radius of curvature R_c. The minimum values of $E/\Delta E_s$, $E/\Delta E_d$ and R_c were tabulated for each configuration.

For the 2x case, the 72 configurations with $E/\Delta E_{s,min} > 200$, $E/\Delta E_{d,min} > 200$ and $R_{c,min} > 20$mm were sorted out. These configurations are plotted as E_{min}, E_{max} points in spectral-range space in Fig.2, assuming an RAP crystal (with Bragg plane spacing $2d = 26.121$Å).

We have a particular interest in the range defined by $E_{min} \leq 1.0$ and $E_{max} \geq 2.0$ keV for upcoming experiments. Fig. 2 indicates that options exist at 2x magification. No option exists at 3x because at this higher magnification the slit entrance position runs into the diagnostic space envelope, limiting the viable volume in $\eta - f - \epsilon$ configuration space. This constraint can be removed if the diagnostic is extended outside the space envelope, but then spatial interferences might preclude use of some adjacent beams.

For the 2x configuration options, a fine-grained parameter scan yields an optimal ellipse with $\eta = 4.6\,\mathrm{deg}$, $f = 174$mm, and $\epsilon = 0.9885$. This is the sample geometry shown in Fig. 1. The resulting crystal mount is 33.8 mm long, 5.1 to 12.7 mm high, and 36.0 mm wide, with a minimum radius of curvature of 25.7 mm. Fig. 3 shows the spectral range of this instrument for three different crystals. This MSPEC-E design has been built and fielded with an RAP crystal, producing a total of 92 film images (4 frames of data on each of 23 shots) at the Omega laser. Both PET and octadecyl hydrogen maleate (OHM) crystals have also been bent to the ellipse.

Fig. 4 shows the predicted contributions to the overall spectral resolution for a relatively large 600μm source. Source broadening is well mitigated by this design. Initial analyses of the spectral dispersion and resolution from are consistent with the design predictions, with

features appearing within 1 mm of their expected location on the MCP, and lines resolved to $E/\Delta E \geq 250 - 700$ over the range 1180 to 1550 eV.

Fig. 5 shows a sample image and lineout from one frame. The target was a glass tube (SiO_2) containing a low-density Zn-doped SiO_2 foam, viewed from 79.2 deg to the axis of the tube, and space-resolved across the long aperture of the tube. We expected to see the Zn L-shell complex, but our initial spectral calibration, based entirely on the instrument geometry, showed no clear Zn features. We were surprised to identify the Na Ly alpha line as the dominant spectral feature, but soon determined that the glass was a borosilicate (Pyrex) having substantial Na content. The spectrum shown here was recalibrated using only the Na line as a reference, and then the Si K-shell lines fell into place. The Si K-shell appears in second order. This is possible, despite the order-of-magnitude lower second-order reflectivity of RAP, because of strong attenuation of first order photons in the filters (a total of 25.4μm of Be). In sum, because of the small amount of Zn in the very low-density foam, the steep viewing angle, and the high abundance of Na in the wall, our signal is dominated by Na and Si features, and we do not identify any Zn features at all (at the gain settings used). But for our instrument-calibration purposes, the K-shell spectra are in fact better than Zn L-shell lines would have been.

Fig. 5 also shows attenuation of the spectrum beyond 1.3 keV. After ruling out Mg contamination in the filters, subsequent investigations determined conclusively that this was due to clipping from a capture plate in the rear filter assembly (near the detector surface). The Omega XRFC rear-filter components were mainly designed for pinhole imaging, and many are not wide enough for spectrometers (which have higher incident angles at the detector). Other spectra have been obtained with spectral coverage from 1.0 to beyond 1.68 keV, with wavelengths calibrated using the K edge of a 2 micron Al filter.

Overall this new instrument appears to be a promising tool for spectroscopic applications requiring time-and-space resolved data with reasonably high spectral resolution over a broad spectral range. An end-to-end relative calibration of the instrument is underway.

Acknowledgments

The authors thank Peter Beiersorfer and Marilyn Schneider for numerous discussions regarding crystal spectroscopy. This work was performed under the auspices of the U.S.

Department of Energy by University of California, Lawrence Livermore National Laboratory under contract W-7405-ENG-48.

---

[1] B. L. Henke, H. T. Yamada, and T. J. Tanaka, Rev. Sci. Instrum. **54**, 1311 (1983).

[2] B. L. Henke and P. A. Jaanimagi, Rev. Sci. Instrum. **56**, 1537 (1985).

[3] B. A. Hammel, D. W. Phillion, and L. E. Ruggles, Rev. Sci. Instrum. **61**, 1920 (1990).

[4] J. E. Bailey, G. A. Chandler, D. Cohen, M. E. Cuneo, M. E. Foord, R. F. Heeter, D. Jobe, P. W. Lake, J. J. MacFarlane, T. J. Nash, et al., Phys. Plasmas **9**, 2186 (2002).

[5] M. J. May, R. F. Heeter, and J. E. Emig, Rev. Sci. Instrum. **99**, 9999 (2004), this issue.

[6] B. L. Henke, E. M. Gullikson, and J. C. Davis, Atomic Data and Nuclear Data Tables **54**, 181 (1993).

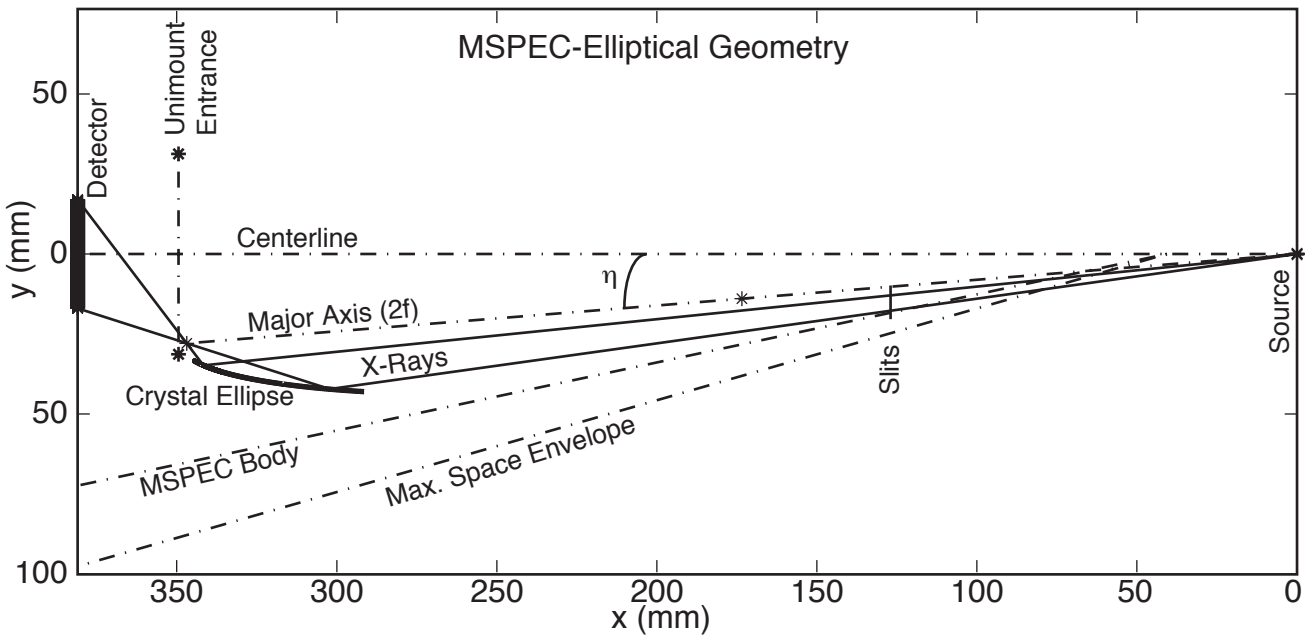

FIG. 1: Geometry for elliptical crystal with face-on detector. The case shown has $\eta = 4.6$ degrees, $2f = 348$ mm, and $\epsilon = 0.9885$.

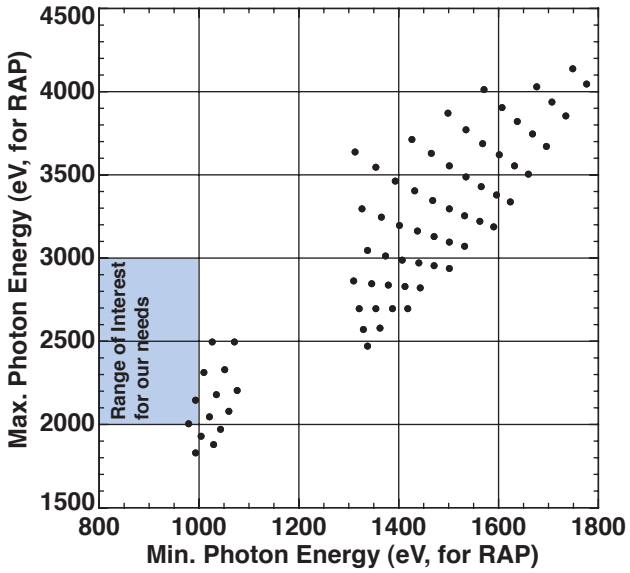

FIG. 2: Spectral ranges of elliptical RAP crystals with $E/\Delta Es, d > 200$ in the MSPEC-2x.

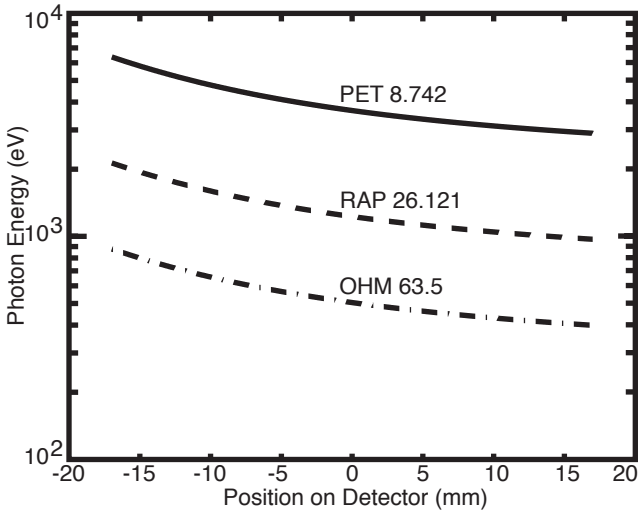

FIG. 3: MSPEC-E spectral ranges for crystals of PET, RAP (fielded), and OHM.

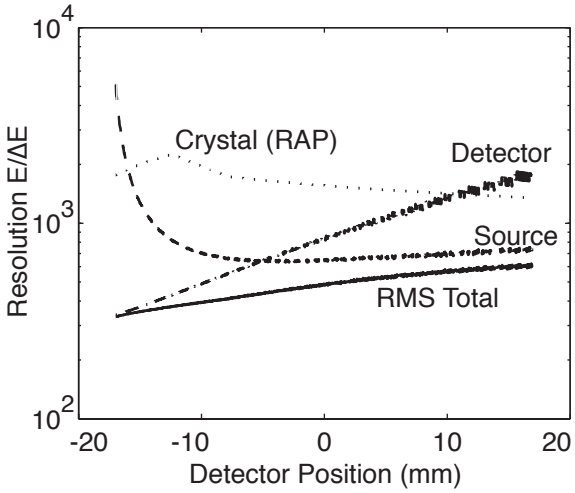

FIG. 4: Overall Spectral Resolution of the MSPEC-E, showing contributions from source broadening (0.6 mm source), detector spatial resolution (0.06 mm effective pixels), and the RAP crystal resolving power [6].

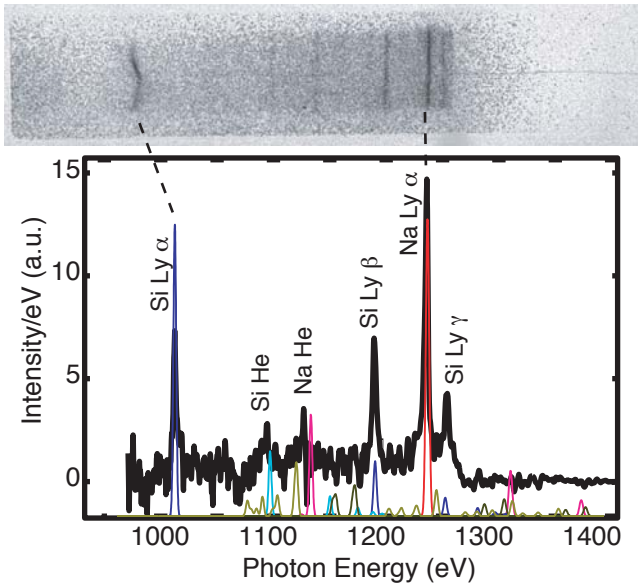

FIG. 5: Top: Sample image from the MSPEC-E. Bottom: Dark line is a lineout of the observed spectrum; light lines are theoretical output indicating line positions (but NOT relative intensities) of K-shell lines of H- and He-like Na (in 1st order) and Si (in 2nd order), which are observed, and also Zn L-shell (1st order) and K-shell (2nd order) lines which are not observed.